Egypt. J. Chem. **Vol. 66**, No. 6, pp. 441 – 455 (2023)

Egyptian Journal of Chemistry

http://ejchem.journals.ekb.eg/

Synthesis, *In Vitro* Biological Investigation, and *In Silico* Analysis of Pyrazole-Based Derivatives as Multi-target Agents

Ashraf S. Hassan [a,*], Wael M. Aboulthana [b]

[a] *Organometallic and Organometalloid Chemistry Department, National Research Centre, Dokki 12622, Cairo, Egypt*

[b] *Biochemistry Department, Biotechnology Research Institute, National Research Centre, Dokki 12622, Cairo, Egypt*

Abstract

The diseases-related complications and causes are threaded. Accordingly, the preparation of one drug with multiple targets is very pressing. In this context, the three series of pyrazole-based derivatives **7a-c, 9a-c,** and **11a-c** were designed and synthesized by using 5-amino-pyrazoles **3a-c** as starting materials. The structures of various products **7a-c**, **9a-c**, and **11a-c** were characterized by using various devices (elemental analysis and spectral tools). The biological activities of pyrazole-based products **7a-c, 9a-c,** and **11a-c** were estimated as antioxidant, anti-diabetic, anti-Alzheimer, and anti-arthritic. The estimation results showed that the two products **7c** and **11a** displayed powerful biological activities. *In silico* analysis (physicochemical, drug-likeness, and toxicity properties) of the two products **7c** and **11a** was performed. This research could be valuable for the exploration of one drug with multiple targets.

Keywords: Pyrazole-based products; Pharmacophore; Physicochemical properties; Anti-diabetic activity; Diseases-related complications

Introduction

Recent epidemiological studies established the relationship between diseases, their complications, and their causes, and also, some diseases' complications lead to other diseases [1, 3]. Diabetes mellitus is characterized by hyperglycemia and insulin resistance. Cardiovascular diseases are the major complication of diabetes [4]. Alzheimer's disease is a neurodegeneration and medicinal studies present that diabetes mellitus and cardiovascular diseases (a complication of diabetes mellitus) are correlated to an increased risk of Alzheimer's disease [5]. The progressive loss of cells and tissues refers to aging. Oxidative stress is the main factor for aging. Also, is responsible for some diseases such as diabetes and Alzheimer's disease. Osteoarthritis, diabetes mellitus, Alzheimer's disease, and cardiovascular disease are famous complications of aging [6]. The diseases-related complications and causes are complex. Therefore, the necessity for cooperation between organic chemistry and medicinal chemistry researchers for the preparation of one drug with multiple targets is very critical for facing diseases the major scourges of humanity [7] **(Figure 1)**.

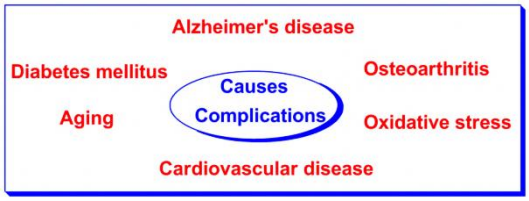

Figure 1: The diseases-related complications and causes

Pyrazole (five-membered ring with two nitrogen atoms) is a pharmacophore moiety. Pyrazole-based derivatives exhibit various biological activities [8-10]. Pyrazole-based Schiff base **I** possessed significant *in vitro* cytotoxic properties against HeLa

*Corresponding author e-mail: ashraf_salmoon@yahoo.com (Ashraf S. Hassan). **ORCID:** https://orcid.org/0000-0002-4771-716X
Received Date: 13 April 2023; Revised Date: 30 April 2023; Accepted Date: 03 May 2023
DOI: 10.21608/ejchem.2023.205639.7863

cells and antibacterial activity against *Salmonella typhimurium* Gram (-) (MIC = 62.5 µg/mL) [11]. Oxadiazol-pyrazole derivative **II** displayed the highest antioxidant assays [12]. Pyrazole derivative which bears a coumarin scaffold **III** showed excellent butyrylcholinesterase inhibitor activity as an anti-Alzheimer agent [13]. Pyrazole-triazole derivative **IV** possesses significant anti-diabetic potency and an inhibitory effect equal to 4.54 nM against the DPP-4 enzyme [14]. Pyrazole sulfonyl derivative **V** is more selective for COX-2 isozyme (anti-inflammatory activity) [15] **(Figure 2)**.

Based on the above-mentioned information about bioactive pyrazole compounds, diseases-related complications, and interferences of the diseases in addition to a continuation of our program for the exploration of bioactive products [16-31], accordingly, we aim in this study to (i) synthesize three series of pyrazole-based derivatives **7a-c, 9a-c,** and **11a-c**. (ii) Estimate the biological activities of pyrazole-based products **7a-c**, **9a-c**, and **11a-c** as antioxidant, anti-diabetic, anti-Alzheimer, and anti-arthritic. (iii) Perform the *in silico* analysis including physicochemical, drug-likeness, and toxicity properties of the biologically potent products.

2. Results and discussion

2.1. Chemistry

5-Amino-1*H*-pyrazole derivatives **3a-c** were prepared according to our prior program, illustrated in **Scheme 1** through the sequential reaction of *N*-aryl-cyanoacetamides **1a-c** with phenyl isothicyanate or 4-methoxyisothicyanate to yield the ketene *N*,*S*-acetals **2a-c** which reacted then with hydrazine hydrate [32, 33]. On the other hand, 4-((4-fluorophenyl)azo)-2-hydroxybenzaldehyde (**6**) [34] was prepared through the coupling between the diazotization of 4-fluoro aniline (**4**) with *2*-hydroxybenzaldehyde (**Scheme 1**). The first series of the target compounds **7a-c** were prepared by the reaction of 5-amino-1*H*-pyrazole derivatives **3a-c** with 4-((4-fluorophenyl)azo)-2-hydroxybenzaldehyde (**6**) (**Scheme 1**).

The compounds structure **7a-c** were characterized via different spectral data. The ^{1}H NMR spectrum data of the **7c** demonstrated four singlet signals for the three NH protons and one OH proton at δ 9.34, 10.22, 11.76, and 13.09 ppm, respectively. Another distinguishing signal at 8.85 ppm for azomethine proton (-CH=N-). The sixteen protons of the four aromatic rings were represented in a range from δ 7.21 to 8.53 ppm. The sixteen protons are exhibited in the ^{1}H NMR spectrum as the following: 7.21-7.28 (multiplet, six protons), 7.42 (triplet, two protons), 7.60 (single, one proton), 7.70-7.73 (multiplet, three protons), 7.88 (triplet, two protons), 8.08 (doublet, one proton with *J* = 6.5 Hz), and 8.53 (single, one proton).

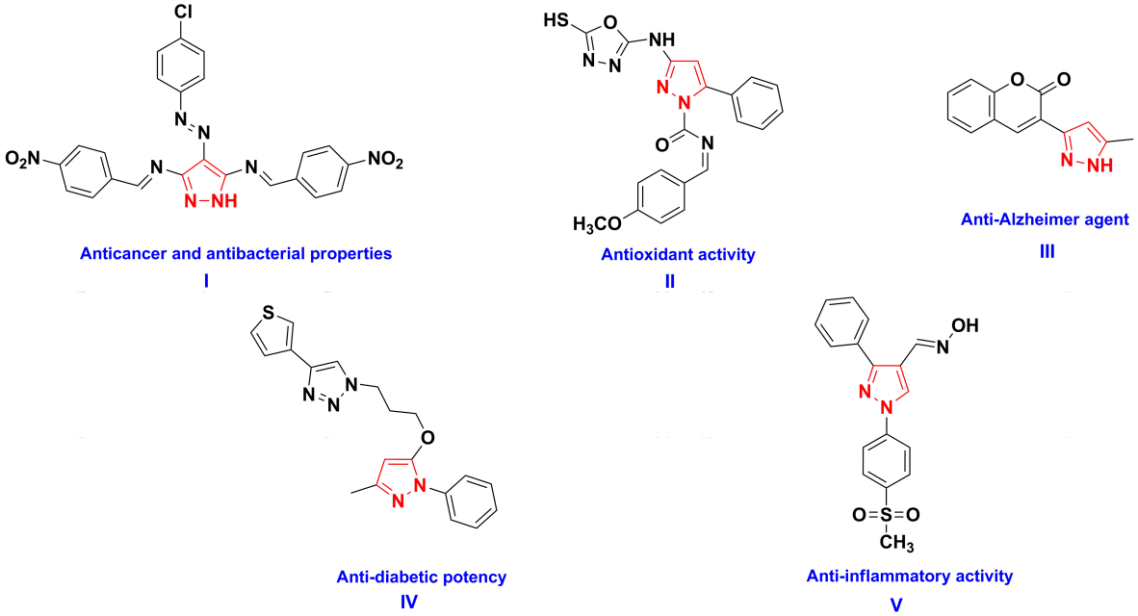

Figure 2: Biological activities of some pyrazole derivatives **I-V**

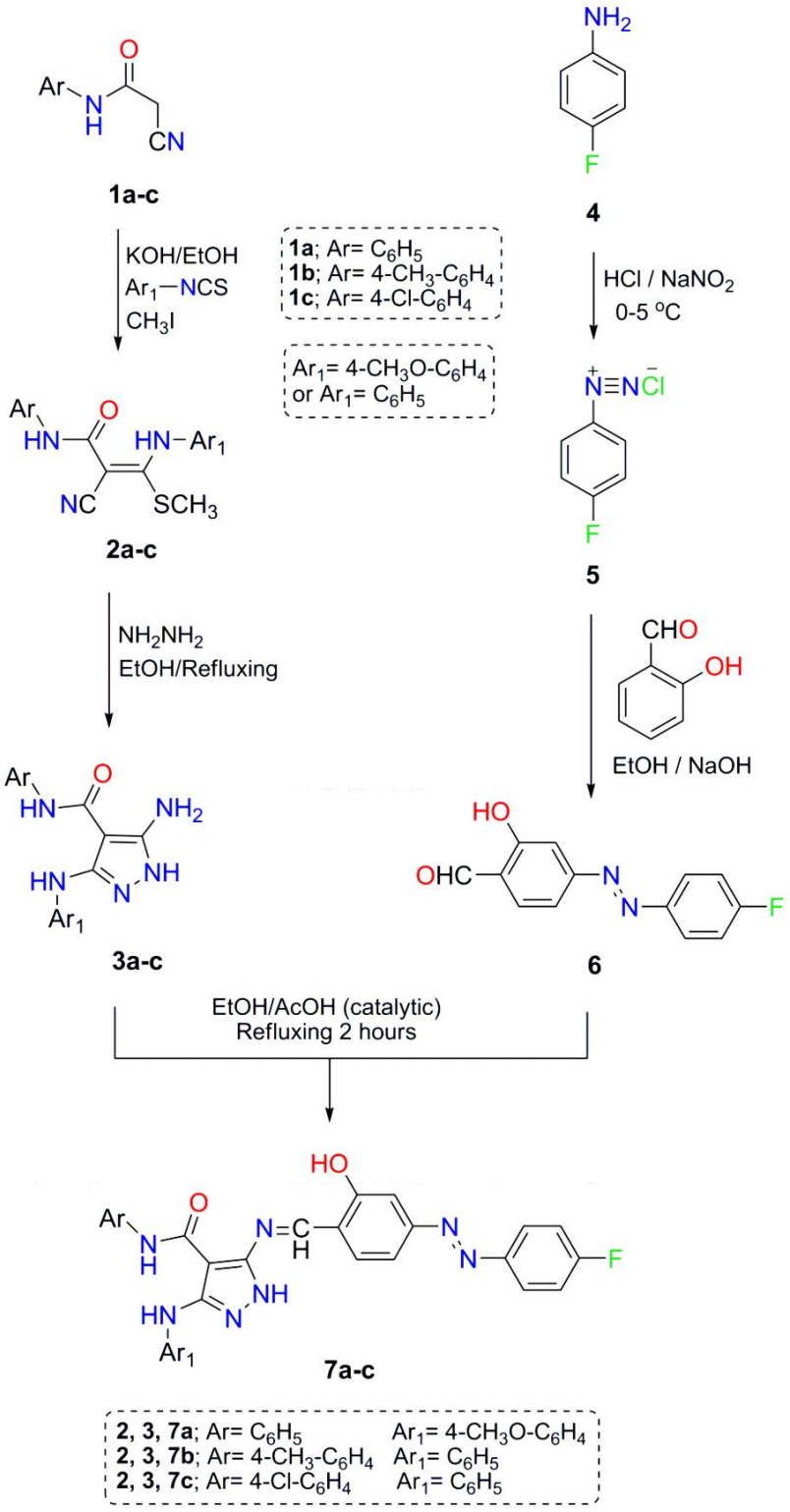

Scheme 1: Synthesis of the first series **7a-c**

The ^{13}C NMR spectrum analysis of **7c** illustrated the carbon atom of carbonyl function (1C, C=O) at δ 164.54 ppm, also, the twenty-seven carbon atoms of aromatic and one carbon atom of the azomethine (-CH=N-) in the range from δ 93.91 to δ 162.74 ppm.

Scheme 2 illustrated the synthesis route of the second and third series of the target compounds **9a-c** and **11a-c**, respectively. The second series **9a-c** was prepared by the reaction of 5-amino-1*H*-pyrazole derivatives **3a-c** with isatin **(8)**. While the third series of the target compounds, pyrazole-based 3-(benzofuran-2-yl)-pyrazole **11a-c**, was prepared *via* the reaction of 5-amino-1*H*-pyrazoles **3a-c** with 3-(benzofuran-2-yl)-1-phenyl-1*H*-pyrazole-4-carbaldehyde **(10)** [35] which was prepared according to literature method by Vilsmeier-Haack reaction.

The structure of the target compounds **9a-c** and **11a-c** was characterized *via* different spectral data. Compound **9a**, taken as a representative example, the ^{1}H NMR analysis of **9a** included that a singlet at δ 3.76 ppm was because of the methoxy protons, whereas the protons of aromatic rings (phenyl, 4-methoxyphenyl, and isatin) were observed as a triplet at δ 6.96 ppm for three protons, multiplet at δ 7.03-7.08 ppm due to two protons, four protons appeared as two doublets: one of them at δ 7.29 (2*H*) with *J* = 8.6 Hz and the other at δ 7.93 (2*H*) with *J* = 7.9 Hz, Two protons as a triplet at *δ* 7.35 ppm, one proton as a triplet at *δ* 7.51 ppm, and finally one proton as a doublet at *δ* 9.08 ppm with *J* = 7.7 Hz. The NH proton of the isatin ring appeared as a singlet at *δ* 13.15 ppm while the three NH protons of the pyrazole moiety appeared as singlets at *δ* 8.79, 11.03, and 11.15 ppm. Also, the ^{13}C NMR analysis of **9a** appears the carbon atom of the methoxy group at *δ* 55.35 ppm, the carbon atoms of the two carbonyls (2C, 2C=O) at *δ* 155.69 and 165.06 ppm, the carbon atom of azomethine function (1C, -C=N-) at *δ* 162.35 ppm, and twenty-one aromatic carbon atoms from *δ* 94.10 to *δ* 150.43 ppm.

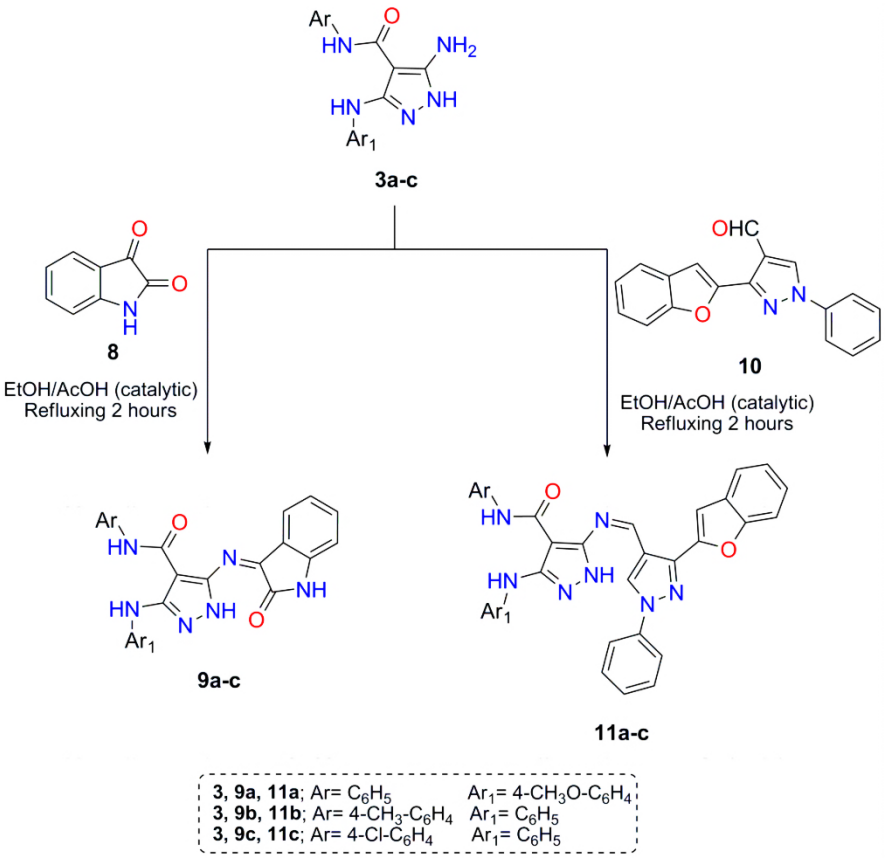

Scheme 2: Synthesis of pyrazole-based derivatives **9a-c** and **11a-c**

2.2. Biological activities evaluation

2.2.1. *In vitro* antioxidant activities

Oxidative stress and free radicals are dangerous to human health and lead to aging and chronic diseases. Antioxidants are compounds that have the ability to control oxidative stress degree; thus, these compounds gained formidable attention from the organic and pharmaceutical researchers [36]. Therefore, the antioxidant activities study of all pyrazole-based derivatives **7a-c**, **9a-c**, and **11a-c** were performed by using four different assays and the results were listed in **Table 1.**

Among all the pyrazole-based derivatives **7a-c, 9a-c,** and **11a-c**, we found that the two compounds **7c** and **11a** registered the most powerful total antioxidant capacity (TAC) equal to 85.15 ± 0.22 and 84.73 ± 0.22 mg gallic acid/gm, respectively. Also, the same two compounds **7c** and **11a** demonstrated the highest iron-reducing power (IRP) with values of 54.19 ± 0.08 and 53.92 ± 0.08 µg/mL, respectively.

The scavenging activities results of the pyrazole-based derivatives **7a-c**, **9a-c**, and **11a-c** against 1, 1-diphenyl-2-picryl-hydrazyl (DPPH) radicals refer to the two most active and more potent compounds **7c** and **11a** with IC_{50} values equal to 8.56 ± 0.01 and 8.60 ± 0.01 µg/ml, respectively, in comparison to ascorbic acid (IC_{50} = 4.10 ± 0.01 µg/ml). Also, the scavenging activities results against 2, 2'-azinobis-(3-ethylbenzothiazoline-6-sulfonic acid) (ABTS) showed the two more effective compounds **7c** and **11a** with percentage values equal to 112.03 ± 0.05 % and 111.48 ± 0.05 %, respectively, in comparison to ascorbic acid (39.10 ± 0.01 %).

From the results of the antioxidant activities and the scavenging activities, we can conclude that the two compounds **7c** and **11a** are the most active and more powerful derivatives among all the pyrazole-based derivatives **7a-c**, **9a-c**, and **11a-c**.

Table 1: The antioxidant activities and scavenging activities of pyrazole-based derivatives **7a-c, 9a-c,** and **11a-c:-**

Pyrazole-based derivatives	**Total antioxidant capacity (TAC)** (mg gallic acid/gm)	**Iron-reducing power (IRP)** (µg/mL)	**Scavenging activity against DPPH** (IC_{50} µg/ml)	**Scavenging activity against ABTS (%)**
7a	39.08 ± 0.10	24.87 ± 0.04	18.65 ± 0.02	51.41 ± 0.02
7b	39.37 ± 0.10	25.05 ± 0.04	18.51 ± 0.02	51.80 ± 0.02
7c*	**85.15 ± 0.22***	**54.19 ± 0.08***	**8.56 ± 0.01***	**112.03 ± 0.05***
9a	42.01 ± 0.11	26.73 ± 0.04	17.35 ± 0.02	55.27 ± 0.03
9b	43.37 ± 0.05	27.68 ± 0.02	16.77 ± 0.02	57.18 ± 0.01
9c	42.72 ± 0.11	27.19 ± 0.04	17.06 ± 0.02	56.21 ± 0.03
11a*	**84.73 ± 0.22**	**53.92 ± 0.08**	**8.60 ± 0.01**	**111.48 ± 0.05**
11b	23.94 ± 0.06	15.24 ± 0.02	30.43 ± 0.04	31.50 ± 0.02
11c	23.73 ± 0.06	15.10 ± 0.02	30.70 ± 0.04	31.23 ± 0.01
Ascorbic Acid	-	-	4.10 ± 0.01	39.10 ± 0.01

* The most effective compound.

Table 2: The anti-diabetic, anti-Alzheimer, and anti-arthritic activities of pyrazole-based derivatives **7a-c, 9a-c,** and **11a-c:-**

Pyrazole-based derivatives	Anti-diabetic Activity		Anti-Alzheimer Activity	Anti-arthritic Activity	
	α-Amylase inhibition (%)	α-Glucosidase inhibition (%)	AChE inhibition (%)	Proteinase Denaturation (%)	Inhibition of Proteinase (%)
7a	70.42 ± 0.03	82.02 ± 0.01	33.65 ± 0.01	72.07 ± 0.02	70.49 ± 0.01
7b	70.95 ± 0.03	81.87 ± 0.01	33.60 ± 0.01	71.94 ± 0.02	70.36 ± 0.01
7c*	**107.27 ± 0.04**	**124.94 ± 0.02**	**51.26 ± 0.02**	**109.79 ± 0.02**	**107.37 ± 0.02**
9a	75.70 ± 0.03	88.17 ± 0.01	36.18 ± 0.01	77.48 ± 0.02	75.77 ± 0.01
9b	78.28 ± 0.02	90.30 ± 0.01	36.43 ± 0.01	78.32 ± 0.03	76.60 ± 0.01
9c	76.99 ± 0.03	89.67 ± 0.01	36.57 ± 0.01	77.47 ± 0.03	75.77 ± 0.01
11a*	**92.13 ± 0.04**	**107.31 ± 0.02**	**38.96 ± 0.02**	**79.57 ± 0.02**	**77.82 ± 0.01**
11b	43.15 ± 0.02	50.26 ± 0.01	20.62 ± 0.01	44.16 ± 0.01	43.19 ± 0.01
11c	42.77 ± 0.02	49.82 ± 0.01	20.44 ± 0.01	43.78 ± 0.01	42.81 ± 0.01
Acarbose	77.57 ± 0.01	56.79 ± 0.01			
Diclofenac Sodium				48.58 ± 0.02	45.83 ± 0.01

* The most effective compound.

Table 3: The physicochemical and drug-likeness of pyrazole-based derivatives **7c** and **11a:-**

	MW	#Rotatable bonds	#H-bond acceptors	#H-bond donors	TPSA	Lipophilicity (MLOGP)
Lipinski's rule	**≤500**	-	**≤10**	**≤5**	-	**≤4.15**
Veber's (GSK) rule	-	**≤10**	-	-	**≤140**	-
Pyrazole-based derivatives						
7c	553.97	9	7	4	127.12	5.00
11a	593.63	10	6	3	122.36	4.30

Table 4: The four toxicity parameters of pyrazole-based derivatives **7c** and **11a:-**

Pyrazole-based derivatives	Toxicity parameters			
	AMES toxicity	hERG I inhibitor	hERG II inhibitor	Hepatotoxicity
7c	No	No	Yes	Yes
11a	No	No	Yes	No

2.2.2. *In vitro* anti-diabetic activity

Diabetes mellitus (DM) is a chronic metabolic disease (pancreatitis) and refers to raised glucose levels [37]. The two enzymes, α-amylase and α-glucosidase, play an essential role in blood glucose levels, where α-amylase enzyme breaks down the carbohydrates into disaccharides while the α-glucosidase enzyme transforms the disaccharides into monosaccharides [38]. Consequently, their inhibition is one of the therapeutic strategies for controlling hyperglycemia [39]. Accordingly, the anti-diabetic activity of all pyrazole-based derivatives **7a-c**, **9a-c**, and **11a-c** were calculated by determining their inhibition percentage of the α-amylase and α-glucosidase enzymes, and the results were listed in **Table 2.**

In the case of the α-amylase enzyme inhibition percentage estimation, the two compounds **7c** (% = 107.27 ± 0.04) and **11a** (% = 92.13 ± 0.04) possessing more potent inhibition percentages than the standard drug used acarbose (% = 77.57 ± 0.01). The three compounds **9b** (% = 78.28 ± 0.02), **9c** (% = 76.99 ± 0.03), and **9a** (% = 75.70 ± 0.03) showed inhibition percentages almost equally the standard drug used acarbose (% = 77.57 ± 0.01). The four compounds **7b**, **7a**, **11b**, and **11c** are fewer activities than the standard drug used acarbose (% = 77.57 ± 0.01).

On the estimation of the inhibition percentages for the α-glucosidase enzyme, we found that the seven derivatives **7a-c**, **9a-c**, and **11a** possess inhibition percentages in the range from 124.94 ± 0.02 to 81.87 ± 0.01 are more active than acarbose (% = 56.79 ± 0.01). While the two compounds **11b** (% = 50.26 ± 0.01) and **11c** (% = 49.82 ± 0.01) show inhibition percentages less than the acarbose (% = 56.79 ± 0.01).

2.2.3. *In vitro* anti-Alzheimer activity

Alzheimer's disease is a progressive neurodegenerative disease distinguished by memory frailty. Based on the reports of the World Health Organization, Alzheimer's disease is one of the diseases and scourges of humanity. Also, is the sixth global death cause [40]. The Alzheimer's patient brain is characterized and demonstrated that acetylcholinesterase (AChE) enzyme is associated with β-amyloid plaques. Hence, inhibition of acetylcholinesterase (AChE) is a therapeutic strategy for controlling Alzheimer's disease [41]. From this, the anti-Alzheimer activity of all pyrazole-based derivatives **7a-c**, **9a-c**, and **11a-c** were calculated by determining the acetylcholinesterase (AChE) enzyme inhibition percentage, and the results were registered in **Table 2**.

The anti-Alzheimer activity result refers to compound **7c** possessing the highest acetylcholinesterase (AChE) enzyme inhibition percentage (AChE inhibition (%) = 51.26 ± 0.02) among all the pyrazole-based derivatives. The next compound in the activity is **11a** with acetylcholinesterase (AChE) enzyme inhibition percentage (AChE inhibition (%)) equal to 38.96 ± 0.02. The order of the inhibition activities for the rest derivatives is **9c** (36.57 ± 0.01 %) > **9b** (36.43 ± 0.01 %) > **9a** (36.18 ± 0.01 %) > **7a** (33.65 ± 0.01 %) > **7b** (33.60 ± 0.01 %) > **11b** (20.62 ± 0.01 %) > **11c** (20.44 ± 0.01 %).

2.2.4. *In vitro* anti-arthritic Activity

Arthritis patients are characterized by the presence of proteinase denaturation and proteinase enzyme in high percentages in the body. Accordingly, the inhibition of the two enzymes, proteinase denaturation, and proteinase enzyme, is a therapeutic strategy for controlling arthritis disease.

The anti-arthritic activities of all pyrazole-based derivatives **7a-c**, **9a-c**, and **11a-c** were calculated by estimating the proteinase denaturation inhibition percentage with proteinase enzyme inhibition percentage. The anti-arthritic activities results were listed in **Table 2**.

All the pyrazole-based derivatives except the two compounds **11b** (PD = 44.16 ± 0.01 %) and **11c** (PD = 43.78 ± 0.01 %) demonstrated proteinase denaturation inhibition percentage (PD, %) in the range from 109.79 ± 0.02 to 71.94 ± 0.02 % more than diclofenac sodium (PD = 48.58 ± 0.02 %).

Also, in the case of inhibition of proteinase percentage (IP, %) determination, the pyrazole-based derivatives **7a-c**, **9a-c**, and **11a** show inhibition percentage higher than diclofenac sodium (IP = 45.83 ± 0.01 %). But the two compounds **11b** and **11c** demonstrated an inhibition percentage less than diclofenac sodium.

Finally, from the above results of biological activities we can found that the two compounds **7c** and **11a** possessing more potent biological activities than the rest derivatives. Maybe the activity of the derivative **7c** is due to the presence of 4-chlorophenyl and 4-fluorophenyl azo rings [42]. Compound **11a** bore pyrazole moiety and another pyrazole attached to benzofuran moiety. The two moieties, pyrazole and benzofuran, maybe the reason that improves the inhibition percentage for the acetylcholinesterase (AChE) enzyme [43].

2.3. *In silico* evaluation analysis

2.3.1. Physicochemical and drug-likeness

The physicochemical and drug-likeness of the two compounds **7c** and **11a** were predicted by utilizing the web http://swissadme.ch/index.php#undefined [44]. The results were demonstrated in **Table 3**.

The results of **Table 3** refer to that (i) the two compounds **7c** and **11a** are not agreed with Lipinski's

rule because the two parameters, the molecular weight (MW) and the lipophilicity (MLOGP), are more than 500 and 4.15, respectively. (ii) The two compounds **7c** and **11a** show agreement with Veber's (GSK) rule (Rotatable bonds ≤ 10 and the total polar surface area (TPSA) ≤ 140).

2.3.2. *In silico* toxicity prediction

The four toxicity parameters of the two compounds **7c** and **11a** were predicted utilizing the web http://biosig.unimelb.edu.au/pkcsm/prediction [45]. The results of the four toxicity parameters are demonstrated in **Table 4**.

Ames test is used to predict the compound that can cause mutations in the DNA. If the result predicts is positive (yes) therefore the chemical is mutagenic and may act as a carcinogen [46]. The two compounds **7c** and **11a** are negative and hence non-mutagenic.

The inhibition of the K (+) channels encoded by hERG is associated with cardiac arrhythmias and then sudden cardiac death. hERG inhibition includes two types: hERG I inhibition and hERG II inhibition. If the result predicts is positive (yes) therefore the compound is an inhibitor [47]. The two compounds **7c** and **11a** are non-inhibitors of the hERG I enzyme. On the other hand, **7c** and **11a** are inhibitors of the hERG II enzyme, therefore causing cardiac arrhythmias.

Hepatotoxicity indicates compound-driven liver damage. If the result predicts is positive (yes) therefore the compound causes acute and chronic liver disease [48]. Compound **7c** has hepatotoxicity and causes liver disease but compound **11a** is safe and not has hepatotoxicity.

3. Conclusions

The three series of pyrazole-based derivatives **7a-c, 9a-c,** and **11a-c** were successfully synthesized. Structures of products **7a-c, 9a-c,** and **11a-c** were characterized and investigated using elemental analysis and different spectral data. The biological properties of the synthesized products **7a-c, 9a-c,** and **11a-c** as one drug with multi-targets were determined and these biological properties include antioxidant, anti-diabetic, anti-Alzheimer, and anti-arthritic. The two products **7c** and **11a** possess more potent biological activities than the rest derivatives as significant antioxidants, inhibitors of acetylcholinesterase (AChE), α-amylase, α-glucosidase, proteinase denaturation, and proteinase enzymes **(Figure 3)**.

Based on *in silico* analysis, the two compounds **7c** and **11a** agree with Veber's rule, are non-mutagenic, non-inhibitors of the hERG I enzyme but inhibitors of the hERG II enzyme. Also, compound **11a** is safe and not has hepatotoxicity.

In the after time, the research venture will be protracted to modify the chemical structure of the two products **7c** and **11a** to obtain one drug with multi-targets.

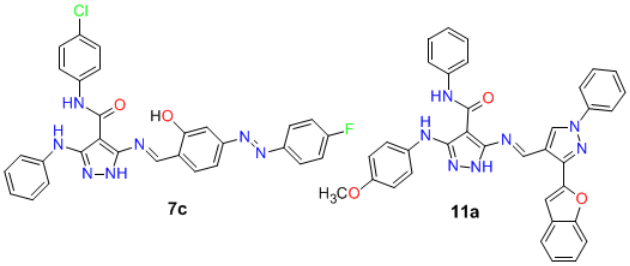

Figure 3: Structures of the two compounds **7c** and **11a**

4. Experimental

4.1. Chemistry

All melting points are incorrect. The Gallenkamp apparatus was used for measuring the melting points.

The JEOL spectrometer was used for ^{1}H NMR (500 MHz) and ^{13}C NMR (125 MHz) spectra. DMSO-d_6 was used as a solvent. For the internal standard (ppm = zero) use TMS. Chemical shifts (δ) and the coupling constants (*J*) were reported in ppm and Hz, respectively.

Elemental analyses were performed at the Microanalytical Center, Cairo University, Egypt.

General procedure for the synthesis of pyrazole-based derivatives 7a-c, 9a-c, or **11a-c**

A mixture of 5-amino-1*H*-pyrazoles **3a-c** (0.01 mol) and 4-((4-fluorophenyl)azo)-2-hydroxybenzaldehyde (**6**) (0.01 mol, 0.244 g), isatin **(8)** (0.01 mol, 0.147g), or 3-(benzofuran-2-yl)-1-phenyl-1*H*-pyrazole-4-carbaldehyde (**10**) (0.01 mol, 0.288 g) in absolute ethanol (25 mL). This mixture reaction was refluxed for two hours. After the reaction was completed and cooled. The target products, pyrazole-based derivatives **7a-c**, **9a-c**, or **11a-c**, respectively, were formed and filtered in the crystals form.

5-(4-((4-Fluorophenyl)azo)-2-hydroxybenzylideneamino)-3-(4-

methoxyphenylamino)-*N*-phenyl-1*H*-pyrazole-4-carboxamide (7a)

Yellow crystals, m.p. = 242-244 °C, yield (82 %). ^{1}H NMR (DMSO-d_6, 500 MHz, δ ppm) 3.70 (s, 3H, OCH_3), 6.88 (d, 2H, *J* = 8.6 Hz, aromatic-H), 7.03 (t, 1H, aromatic-H), 7.17-7.23 (m, 4H, aromatic-H), 7.37-7.41 (m, 3H, aromatic-H), 7.70 (d, 2H, *J* = 7.8 Hz, aromatic-H), 7.85-7.87 (m, 2H, aromatic-H), 8.01 (d, 1H, *J* = 9.1 Hz, aromatic-H), 8.54 (s, 1H, aromatic-H), 8.68 (s, 1H, -CH=N-, azomethine). 9.37 (s, 1H, NH), 10.14 (s, 1H, NH), 11.69 (s, 1H, NH), 13.05 (s, 1H, OH). ^{13}C NMR (DMSO-d_6, 125 MHz, δ ppm) 55.78 (1C, OCH_3), 93.14, 114.81, 114.98, 116.71, 116.89, 117.74, 118.49, 119.47, 120.31, 122.26, 123.71, 124.94, 125.02, 129.11, 129.43, 129.79, 139.26, 145.39, 149.33, 162.98, 163.06, 163.38 (28C, 27C of aromatic + 1C of azomethine -CH=N-), 165.04 (1C, C=O). Anal. Calcd. (%) for $C_{30}H_{24}FN_7O_3$ (549.56): C, 65.57; H, 4.40; N, 17.84. Found: C, 65.64; H, 4.35; N, 17.90 %.

5-(4-((4-Fluorophenyl)azo)-2-hydroxybenzylideneamino)-3-(phenylamino)-*N*-(4-methylphenyl)-1*H*-pyrazole-4-carboxamide (7b)

Yellow crystals, m.p. = 225-227 °C, yield (79 %). ^{1}H NMR (DMSO-d_6, 500 MHz, δ ppm) 2.21 (s, 3H, CH_3), 6.86 (s, 1H, aromatic-H), 7.01 (d, 2H, *J* = 8.1 Hz, aromatic-H), 7.14-7.20 (m, 2H, aromatic-H), 7.41 (t, 2H, aromatic-H), 7.54 (d, 2H, *J* = 8.1 Hz, aromatic-H), 7.58 (d, 2H, *J* = 8.6 Hz, aromatic-H), 7.86-7.88 (m, 3H, aromatic-H), 8.03 (d, 1H, *J* = 6.2 Hz, aromatic-H), 8.54 (d, 1H, *J* = 2.4 Hz, aromatic-H), 8.92 (s, 1H, -CH=N-, azomethine). 9.34 (s, 1H, NH), 10.09 (s, 1H, NH), 11.64 (s, 1H, NH), 13.02 (s, 1H, OH). Anal. Calcd. (%) for $C_{30}H_{24}FN_7O_2$ (533.56): C, 67.53; H, 4.53; N, 18.38. Found: C, 67.48; H, 4.59; N, 18.31 %.

***N*-(4-Chlorophenyl)-5-(4-((4-fluorophenyl)azo)-2-hydroxybenzylideneamino)-3-(phenylamino)-1*H*-pyrazole-4-carboxamide (7c)**

Yellow crystals, m.p. = 240-242 °C, yield (75 %). ^{1}H NMR (DMSO-d_6, 500 MHz, δ ppm) 7.21-7.28 (m, 6H, aromatic-H), 7.42 (t, 2H, aromatic-H), 7.60 (s, 1H, aromatic-H), 7.70-7.73 (m, 3H, aromatic-H), 7.88 (t, 2H, aromatic-H), 8.08 (d, 1H, *J* = 6.5 Hz, aromatic-H), 8.53 (s, 1H, aromatic-H), 8.85 (s, 1H, -CH=N-, azomethine). 9.34 (s, 1H, NH), 10.22 (s, 1H, NH), 11.76 (s, 1H, NH), 13.09 (s, 1H, OH). ^{13}C NMR (DMSO-d_6, 125 MHz, δ ppm) 93.91, 111.81, 116.23, 116.41, 117.96, 120.66, 121.62, 121.83, 124.54, 124.61, 126.78, 128.78, 128.93, 129.11, 129.70, 137.51, 144.92, 148.77, 158.93, 162.32, 162.56, 162.74 (28C, 27C of aromatic + 1C of azomethine -CH=N-), 164.54 (1C, C=O). Anal. Calcd. (%) for $C_{29}H_{21}ClFN_7O_2$ (553.97): C, 62.87; H, 3.82; N, 17.70. Found: C, 62.95; H, 3.76; N, 17.64 %.

3-(4-Methoxyphenylamino)-5-(2-oxoindolin-3-ylideneamino)-*N*-phenyl-1*H*-pyrazole-4-carboxamide (9a)

Dark green crystals, m.p. > 280 °C, yield (82 %). ^{1}H NMR (DMSO-d_6, 500 MHz, δ ppm) 3.76 (s, 3H, OCH_3), 6.96 (t, 3H, aromatic-H), 7.03-7.08 (m, 2H, aromatic-H), 7.29 (d, 2H, *J* = 8.6 Hz, aromatic-H), 7.35 (t, 2H, aromatic-H), 7.51 (t, 1H, aromatic-H), 7.93 (d, 2H, *J* = 7.9 Hz, aromatic-H), 8.79 (s, 1H, NH), 9.08 (d, 1H, *J* = 7.7 Hz, aromatic-H), 11.03 (s, 1H, NH), 11.15 (s, 1H, NH), 13.15 (s, 1H, NH, isatin). ^{13}C NMR (DMSO-d_6, 125 MHz, *δ* ppm) 55.35 (1C, OCH_3), 94.10, 111.26, 114.78, 117.11, 118.49, 121.88, 121.97, 122.88, 128.93, 129.73, 132.11, 135.91, 139.28, 148.18, 148.63, 149.67, 150.43 (21C), 155.69 (1C, C=O), 162.35 (1C, C=N), 165.06 (1C, C=O). Anal. Calcd. (%) for $C_{25}H_{20}N_6O_3$ (452.46): C, 66.36; H, 4.46; N, 18.57. Found: C, 66.40; H, 4.41; N, 18.62 %.

5-(2-Oxoindolin-3-ylideneamino)-3-(phenylamino)-*N*-(4-methylphenyl)-1*H*-pyrazole-4-carboxamide (9b)

Dark brown crystals, m.p. > 280 °C, yield (85 %). ^{1}H NMR (DMSO-d_6, 500 MHz, δ ppm) 2.27 (s, 3H, CH_3), 6.97 (d, 1H, *J* = 8.1 Hz, aromatic-H), 7.04-7.08 (m, 2H, aromatic-H), 7.15 (d, 2H, *J* = 8.7 Hz, aromatic-H), 7.31 (d, 2H, *J* = 8.3 Hz, aromatic-H), 7.37 (t, 2H, aromatic-H), 7.51 (t, 1H, aromatic-H), 7.82 (d, 2H, *J* = 8.7 Hz, aromatic-H), 9.06 (s, 1H, NH), 9.09 (d, 1H, *J* = 8.2 Hz, aromatic-H), 11.02 (s, 1H, NH), 11.10 (s, 1H, NH), 13.43 (s, 1H, NH, isatin). ^{13}C NMR (DMSO-d_6, 125 MHz, *δ* ppm) 20.42 (1C, CH_3), 95.31, 111.19, 116.38, 117.06, 118.26, 118.53, 121.88, 128.88, 129.20, 129.51, 131.81, 135.83, 136.65, 141.10, 147.18, 148.17, 149.61 (21C), 152.13 (1C, C=O), 162.03 (1C, C=N), 164.97 (1C, C=O). Anal. Calcd. (%) for $C_{25}H_{20}N_6O_2$ (436.47): C, 68.80; H, 4.62; N, 19.25. Found: C, 68.73; H, 4.69; N, 19.18 %.

***N*-(4-Chlorophenyl)-5-(2-oxoindolin-3-ylideneamino)-3-(phenylamino)-1*H*-pyrazole-4-carboxamide (9c)**

Dark brown crystals, m.p. > 280 °C, yield (80 %). ^{1}H NMR (DMSO-d_6, 500 MHz, δ ppm) 6.96 (d, 1H, *J* = 7.9 Hz, aromatic-H), 7.06 (t, 2H, aromatic-H), 7.31 (d, 2H, *J* = 8.1 Hz, aromatic-H), 7.35-7.42 (m, 4H, aromatic-H), 7.51 (t, 1H, aromatic-H), 7.95 (d, 2H, *J* = 9.2 Hz, aromatic-H), 9.00 (s, 1H, NH), 9.07 (d, 1H, *J* = 8.7 Hz, aromatic-H), 11.02 (s, 1H, NH), 11.35 (s, 1H, NH), 13.44 (s, 1H, NH, isatin). Anal. Calcd. (%) for $C_{24}H_{17}ClN_6O_2$ (456.88): C, 63.09; H, 3.75; N, 18.39. Found: C, 63.15; H, 3.69; N, 18.50 %.

5-((3-(Benzofuran-2-yl)-1-phenyl-1*H*-pyrazol-4-yl)methyleneamino)-3-(4-methoxyphenylamino)-*N*-phenyl-1*H*-pyrazole-4-carboxamide (11a)

Yellow crystals, m.p. = 261-263 °C, yield (85 %). ^{1}H NMR (DMSO-d_6, 500 MHz, δ ppm) 3.70 (s, 3H, OCH_3), 6.88 (d, 2H, *J* = 8.1 Hz, aromatic-H), 7.00 (t, 1H, aromatic-H), 7.23-7.29 (m, 3H, aromatic-H), 7.37 (t, 1H, aromatic-H), 7.45 (t, 2H, aromatic-H), 7.59-7.70 (m, 8H, aromatic-H), 8.04 (d, 2H, *J* = 7.7 Hz, aromatic-H), 8.74 (s, 1H, -CH=N-, azomethine), 9.29 (s, 1H, NH), 9.51 (s, 1H, pyrazole H-5), 9.74 (s, 1H, NH), 10.13 (s, 1H, NH). ^{13}C NMR (DMSO-d_6, 125 MHz, *δ* ppm) 55.79 (1C, OCH_3), 92.17, 107.17, 111.99, 114.97, 119.96, 120.04, 120.32, 122.24, 123.69, 124.09, 126.01, 128.51, 129.27, 130.33, 131.42, 137.88, 138.21, 139.01, 139.17, 144.36, 147.46, 148.89, 150.43, 151.33, 154.99 (32C), 161.43 (1C, C=N), 163.39 (1C, C=O). Anal. Calcd. (%) for $C_{35}H_{27}N_7O_3$ (593.63): C, 70.81; H, 4.58; N, 16.52. Found: C, 70.88; H, 4.51; N, 16.48 %.

5-((3-(Benzofuran-2-yl)-1-phenyl-1*H*-pyrazol-4-yl)methyleneamino)-3-(phenylamino)-*N*-(4-methylphenyl)-1*H*-pyrazole-4-carboxamide (11b)

Yellow crystals, m.p. = 240-242 °C, yield (82 %). ^{1}H NMR (DMSO-d_6, 500 MHz, δ ppm) 2.24 (s, 3H, CH_3), 6.89 (s, 1H, aromatic-H), 7.08 (d, 2H, *J* = 8.0 Hz, aromatic-H), 7.28-7.32 (m, 3H, aromatic-H), 7.41 (t, 1H, aromatic-H), 7.47-7.53 (m, 4H, aromatic-H), 7.63-7.75 (m, 6H, aromatic-H), 8.07 (d, 2H, *J* = 7.8 Hz, aromatic-H), 9.01 (s, 1H, -CH=N-, azomethine), 9.29 (s, 1H, NH), 9.56 (s, 1H, pyrazole H-5), 9.69 (s, 1H, NH), 10.22 (s, 1H, NH). ^{13}C NMR (DMSO-d_6, 125 MHz, *δ* ppm) 21.10 (1C, CH_3), 93.23, 106.77, 107.93, 111.55, 116.54, 119.45, 119.60, 119.75, 121.77, 123.61, 125.55, 128.00, 128.06, 129.09, 129.17, 129.87, 130.97, 132.30, 135.85, 138.61, 141.15, 143.90, 148.22, 151.29, 152.35, 154.46 (32C), 161.64 (1C, C=N), 162.68 (1C, C=O). Anal. Calcd. (%) for $C_{35}H_{27}N_7O_2$ (577.63): C, 72.78; H, 4.71; N, 16.97. Found: C, 72.80; H, 4.67; N, 17.02 %.

5-((3-(Benzofuran-2-yl)-1-phenyl-1*H*-pyrazol-4-yl)methyleneamino)-*N*-(4-chlorophenyl)-3-(phenylamino)-1*H*-pyrazole-4-carboxamide (11c)

Yellow crystals, m.p. = 259-261 °C, yield (74 %). ^{1}H NMR (DMSO-d_6, 500 MHz, δ ppm) 6.87 (s, 1H, aromatic-H), 7.26-7.30 (m, 5H, aromatic-H), 7.37 (t, 1H, aromatic-H), 7.46 (t, 2H, aromatic-H), 7.60-7.71 (m, 8H, aromatic-H), 8.03 (d, 2H, *J* = 7.7 Hz, aromatic-H), 8.92 (s, 1H, -CH=N-, azomethine), 9.27 (s, 1H, NH), 9.53 (s, 1H, pyrazole H-5), 9.79 (s, 1H, NH), 10.19 (s, 1H, NH). Anal. Calcd. (%) for $C_{34}H_{24}ClN_7O_2$ (598.05): C, 68.28; H, 4.04; N, 16.39. Found: C, 68.35; H, 3.98; N, 16.43 %.

4.2. Biological activities evaluation

4.2.1. *In vitro* antioxidant activities

4.2.1.1. Total antioxidant capacity (TAC) was performed by employing the method depicted by Prieto *et al* [49].

4.2.1.2. Iron-reducing power was estimated by utilizing the method proposed [50].

4.2.1.3. 1, 1-Diphenyl-2-picryl-hydrazyl (DPPH) radical-scavenging activity was tested by the reported procedure [51].

4.2.1.4. 2, 2'-Azinobis-(3-ethylbenzothiazoline-6-sulfonic acid) (ABTS) radical-scavenging activity was performed based on the method modified [52].

4.2.2. Anti-diabetic activity

The anti-diabetic activities were performed through the determination of the α-amylase inhibition percentage and α-glucosidase inhibition percentage [53].

4.2.3. Anti-Alzheimer activity

The anti-Alzheimer activity was estimated by computing the acetylcholinesterase enzyme inhibition percentage through utilizing the method proposed [54].

4.2.4. Anti-arthritic activities

4.2.4.1. The percentage inhibition of protein denaturation was estimated based on the methods described previously [55-57].

4.2.4.2. Proteinase inhibitory test was performed by computing the inhibition percentage by the method recommended [58].

4.3. *In silico* evaluation analysis

4.4.1. Physicochemical and drug-likeness. The physicochemical and drug-likeness of the two compounds **7c** and **11a** were predicted by utilizing the web http://swissadme.ch/index.php#undefined [44, 59-61].

4.4.2. *In silico* toxicity prediction. The four toxicity parameters of the two compounds **7c** and **11a** were predicted by utilizing the web http://biosig.unimelb.edu.au/pkcsm/prediction [45].

Conflict of interest

The authors declare that they have no competing interests.

Acknowledgments:

The authors thank National Research Centre for the financial support.

References

[1] **Carvalho, C. and Moreira, P.I.,** Metabolic defects shared by Alzheimer's disease and diabetes: A focus on mitochondria. *Curr. Opin. Neurobiol.*, **79**, 102694 (2023). https://doi.org/10.1016/j.conb.2023.102694

[2] **Sharma, V. and Mehdi, M.M.,** Oxidative stress, inflammation and hormesis: The role of dietary and lifestyle modifications on aging. *Neurochem. Int.*, **164**, 105490 (2023). https://doi.org/10.1016/j.neuint.2023.105490

[3] **Abdelhamid, R.F. and Nagano, S.,** Crosstalk between Oxidative Stress and Aging in Neurodegeneration Disorders. *Cells* **12** (5), 753 (2023). https://doi.org/10.3390/cells12050753

[4] **Touyz, R.M., Camargo, L.L., Rios, F.J., Alves-Lopes, R., Neves, K.B., Guzik, T., Petrie, J. and Montezano, A.C.,** Molecular Mechanisms Underlying Vascular Disease in Diabetes. In: Berbari, A.E., Mancia, G. (eds) Blood Pressure Disorders in Diabetes Mellitus. Updates in Hypertension and Cardiovascular Protection. *Springer, Cham.* (2023) https://doi.org/10.1007/978-3-031-13009-0_7

[5] **Waigi, E.W., Webb, R.C., Moss, M.A., Uline, M.J., McCarthy, C.G. and Wenceslau, C. F.**, Soluble and insoluble protein aggregates, endoplasmic reticulum stress, and vascular dysfunction in Alzheimer's disease and cardiovascular diseases. *GeroScience*, Accepted (2023) https://doi.org/10.1007/s11357-023-00748-y

[6] **Liguori, I., Russo, G., Curcio, F., Bulli, G., Aran, L., Della-Morte, D., Gargiulo, G., Testa, G., Cacciatore, F., Bonaduce, D. and Abete, P.,** Oxidative stress, aging, and diseases. *Clin Interv Aging* **13**, 757-772 (2018). https://doi.org/10.2147/CIA.S158513

[7] **Ramsay, R.R., Popovic-Nikolic, M.R., Nikolic, K., Uliassi, E. and Bolognesi, M.L.,** A perspective on multi-target drug discovery and design for complex diseases. *Clin Transl Med.*, **7** (1), e3 (2018). https://doi.org/10.1186/s40169-017-0181-2

[8] **Ardevines, S., Marqués-López, E. and Herrera, R.P.,** Heterocycles in Breast Cancer Treatment: The Use of Pyrazole Derivtives. *Curr. Med. Chem.*, **30** (10), 1145-1174 (2023). https://doi.org/10.2174/0929867329666220829091830

[9] **Ayman, R., Radwan, A.M., Elmetwally, A.M., Ammar, Y.A. and Ragab, A.,** Discovery of novel pyrazole and pyrazolo[1,5-*a*]pyrimidine derivatives as cyclooxygenase inhibitors (COX-1 and COX-2) using molecular modeling simulation. *Arch. Pharm.* **356** (2), 2200395, 2023. https://doi.org/10.1002/ardp.202200395

[10] **Ansari, A., Ali, A., Asif, M. and Shamsuzzaman.,** Review: biologically active pyrazole derivatives**.** *New J. Chem.***, 41** (1)**,** 16-41 (2017). 10.1039/C6NJ03181A

[11] **Şener, N., Özkinali, S., Altunoglu, Y.C., Yerlikaya, S., Gökçe, H., Zurnaci, M., Gür, M., Baloglu, M.C. and Şener, İ.,** Antiproliferative properties and structural analysis of newly synthesized Schiff bases bearing pyrazole derivatives and molecular docking studies. *J. Mol. Struct.*, **1241**, 130520, (2021). https://doi.org/10.1016/j.molstruc.2021.130520

[12] **Reddy, G.M., Zyryanov, G.V., Basha, N.M., Munagapati, V.S., Wen, J.-C., Gollakota, A.R.K., Shu, C.-M. and Venkatesh, B.C.,** Synthesis of pyrazole tethered oxadiazole and their analogs as potent antioxidant agents. *J.*

Heterocycl. Chem., **59** (11), 1879-1887 (2022). https://doi.org/10.1002/jhet.4523

[13] **Benazzouz-Touami, A., Chouh, A., Halit, S., Terrachet-Bouaziz, S., Makhloufi-Chebli, M., Ighil-Ahriz, K. and Silva, A.M.S.**, New Coumarin-Pyrazole hybrids: Synthesis, Docking studies and Biological evaluation as potential cholinesterase inhibitors. *J. Mol. Struct.*, **1249,** 131591 (2022). https://doi.org/10.1016/j.molstruc.2021.131591

[14] **Nidhar, M., Khanam, S., Sonker, P., Gupta, P., Mahapatra, A., Patil, S., Yadav, B.K., Singh, R.K. and Tewari, A. K.,** Click inspired novel pyrazole-triazole-persulfonimide & pyrazole-triazole-aryl derivatives; Design, synthesis, DPP-4 inhibitor with potential anti-diabetic agents. *Bioorg. Chem.*, **120**, 105586, (2022). https://doi.org/10.1016/j.bioorg.2021.105586

[15] **Fadaly, W.A., Elshaier, Y.A., Nemr, M.T. and Abdellatif, K.R.,** Design, synthesis, modeling studies and biological evaluation of pyrazole derivatives linked to oxime and nitrate moieties as nitric oxide donor selective COX-2 and aromatase inhibitors with dual anti-inflammatory and anti-neoplastic activities. *Bioorg. Chem.*, **134**, 106428 (2023). https://doi.org/10.1016/j.bioorg.2023.106428

[16] **Hassan, A.S., Morsy, N.M., Aboulthana, W.M. and Ragab, A.,** Exploring a novel of isatin-based Schiff bases as multi-target agents: design, synthesis, in vitro biological evaluation, and in silico ADMET analysis with molecular modeling simulations. *RSC Adv.*, **13** (14), 9281-9303 (2023). https://doi.org/10.1039/D3RA00297G

[17] **Khatab, T.K. and Ashraf S. Hassan.** Computational molecular docking and in silico ADMET prediction studies of pyrazole derivatives as COVID-19 main protease (M^{pro}) and papain-like protease (PL^{pro}) inhibitors. *Bull. Chem. Soc. Ethiop*., **37** (2), 449-461 (2023). https://dx.doi.org/10.4314/bcse.v37i2.14

[18] **Mukhtar, S.S., Saleh, F.M., Hassaneen, H.M., Hafez, T.S., Hassan, A.S., Morsy, N.M. and Teleb, M.A.M.,** Synthesis, reaction, antimicrobial, and docking study of new chalcones incorporating isoquinoline moiety. *Synth. Commun*., **52** (19-20), 1909-1916 (2022). https://doi.org/10.1080/00397911.2022.2119415

[19] **Mukhtar, S.S., Morsy, N.M., Hassan, A.S., Hafez, T.S., Hassaneen, H.M. and Saleh, F.M.,** A Review of Chalcones: Synthesis, Reactions, and Biological Importance. *Egypt. J. Chem*., **65** (8), 379-395 (2022). http://10.0.84.104/ejchem.2022.112735.5125

[20] **Hassan, A.S., Morsy, N.M., Aboulthana, W.M. and Ragab, A.,** *In vitro* enzymatic evaluation of some pyrazolo[1,5-*a*]pyrimidine derivatives: design, synthesis, antioxidant, anti-diabetic, anti-Alzheimer, and anti-arthritic activities with molecular modeling simulation. *Drug Dev. Res.*, **84** (1), 3-24 (2023). https://doi.org/10.1002/ddr.22008

[21] **Elgiushy, H.R., Mohamed, S.H., Taha, H., Sawaf, H., Hassan, Z., Abou-Taleb, N.A., El-labbad, E.M., Hassan, A.S., Abouzid, K.A.M. and Hammad, S.F.,** Identification of a promising hit from a new series of pyrazolo[1,5-*a*]pyrimidine based compounds as a potential anticancer agent with potent CDK1 inhibitory and pro-apoptotic properties through a multistep *in vitro* assessment. *Bioorg. Chem*., **120**, 105646 (2022) https://doi.org/10.1016/j.bioorg.2022.105646

[22] **Abdelghany, A.M., Khatab, T.K. and Hassan. A.S.,** Copper-based glass-ceramic as an efficient catalyst in the synthesis of pyrazolo[1,5-*a*]pyrimidine under solvent-free condition with docking validation as COVID-19 main protease (M^{pro}) inhibitor. *Bull. Chem. Soc. Ethiop*., **35** (1), 185-196 (2021). https://dx.doi.org/10.4314/bcse.v35i1.16

[23] **Hassan, A.S.,** Mixed isatin with 3-(2-(aryl)hydrazono)acetylacetone Mn(II), Co(II) and Ni(II) complexes: antibacterial evaluation and molecular properties prediction. *Bull. Chem. Soc. Ethiop*., **34** (3), 533-541 (2020). https://dx.doi.org/10.4314/bcse.v34i3.9

[24] **Mukhtar, S.S., Hassan, A.S., Morsy, N.M., Hafez, T.S., Hassaneen, H.M. and Saleh, F.M.,** Overview on Synthesis, Reactions, Applications, and Biological Activities of Schiff Bases. *Egypt. J. Chem*., **64** (11), 6541-6554 (2021). 10.21608/ejchem.2021.79736.3920

[25] **Morsy, N.M., Hassan, A.S., Hafez, T.S., Mahran, M.R.H., Sadawe, I.A. and Gbaj, A.M.,** Synthesis, antitumor activity, enzyme assay, DNA binding and molecular docking of Bis-Schiff bases of pyrazoles. *J. Iran. Chem. Soc.*, **18** (1), 47-59 (2021). https://doi.org/10.1007/s13738-020-02004-y

[26] **Mukhtar, S.S., Hassan, A.S., Morsy, N.M., Hafez, T.S., Saleh, F.M. and Hassaneen, H.M.,** Design, synthesis, molecular predication and biological evaluation of pyrazole-azomethine conjugates as antimicrobial agents. *Synth. Commun*., **51** (10), 1564-1580 (2021). https://doi.org/10.1080/00397911.2021.1894338

[27] **Hassan, A.S., Osman, S.A. and Hafez, T.S.,** 5-Phenyl-2-furaldehyde: synthesis, reactions and biological activities. *Egypt. J. Chem*., **58** (2), 113-139 (2015). https://doi.org/10.21608/ejchem.2015.978

[28] **Naglah, A.M., Askar, A.A., Hassan, A.S., Khatab, T.K., Al -Omar, M.A. and Bhat, M.A.,** Biological evaluation and molecular docking with *in silico* physicochemical, pharmacokinetic and toxicity prediction of pyrazolo[1,5-*a*]pyrimidines. *Molecules*, **25** (6), 1431 (2020). https://doi.org/10.3390/molecules25061431

[29] **Hassan, A.S. and Hafez, T.S.,** Antimicrobial activities of ferrocenyl complexes: A review. *J. App. Pharm. Sci*., **8** (5), 156-165 (2018). https://doi.org/10.7324/JAPS.2018.8522

[30] **Hassan, A.S., Masoud, D.M., Sroor, F.M. and Askar, A.A.,** Synthesis and biological evaluation of pyrazolo[1,5-*a*]pyrimidine-3-carboxamide as antimicrobial agents. *Med. Chem. Res*., **26** (11), 2909-2919 (2017). https://doi.org/10.1007/s00044-017-1990-y

[31] **Hassan, A.S., Moustafa, G.O., Morsy, N.M., Abdou, A.M. and Hafez, T.S.,** Design, Synthesis and antibacterial activity of *N*-aryl-3-(arylamino)-5-(((5-substituted furan-2-yl)methylene)amino)-1*H*-pyrazole-4-carboxamide as Nitrofurantoin® analogues. *Egypt. J. Chem*., **63** (11), 4469-4481 (2020). https://doi.org/10.21608/ejchem.2020.26158.2525

[32] **Khatab, T.K., Hassan, A.S. and Hafez, T.S.,** V_2O_5/SiO_2 as an efficient catalyst in the synthesis of 5-aminopyrazole derivatives under solvent free condition. *Bull. Chem. Soc. Ethiop*., **33** (1), 135-142 (2019). https://dx.doi.org/10.4314/bcse.v33i1.13

[33] **Hassan, A.S., Hafez, T.S. and Osman, S.A.,** Synthesis, Characterization, and Cytotoxicity of Some New 5-Aminopyrazole and Pyrazolo[1,5-*a*]pyrimidine Derivatives. *Sci. Pharm.*, ***83***, 27-39 (2015). https://doi.org/10.3797/scipharm.1409-14

[34] **Kaur, H., Lim, S.M., Ramasamy, K., Vasudevan, M., Shah, S.A.A. and Narasimhan, B.** Diazenyl Schiff bases: Synthesis, spectral analysis, antimicrobial studies and cytotoxic activity on human colorectal carcinoma cell line (HCT-116). *Arab. J. Chem.*, **13** (1), 377-392 (2020). https://doi.org/10.1016/j.arabjc.2017.05.004

[35] **Baashen, M.A., Abdel-Wahab, B.F. and El-Hiti, G.A.,** A simple procedure for the synthesis of novel 3-(benzofur-2-yl)pyrazole-based heterocycles. *Chem. Pap.*, **71**, 2159-2166 (2017). https://doi.org/10.1007/s11696-017-0209-5

[36] **Pizzino, G., Irrera, N., Cucinotta, M., Pallio, G., Mannino, F., Arcoraci, V., Squadrito, F., Altavilla, D. and Bitto, A.,** Oxidative Stress: Harms and Benefits for Human Health. *Oxid. Med. Cell Longev.*, **2017**, 8416763 (2017). https://doi.org/10.1155/2017/8416763

[37] **Kozieł, K. and Urbanska, E.M.** Kynurenine Pathway in Diabetes Mellitus-Novel Pharmacological Target?. *Cells* **12**, 460 (2023). https://doi.org/10.3390/cells12030460

[38] **Alqahtani, A.S., Hidayathulla, S., Rehman, M.T., ElGamal, A.A., Al-Massarani, S., Razmovski-Naumovski V., Alqahtani, M.S., El Dib, R.A. and AlAjmi, M.F.,** Alpha-Amylase and Alpha-Glucosidase Enzyme Inhibition and Antioxidant Potential of 3-Oxolupenal and Katononic Acid Isolated from *Nuxia oppositifolia*. *Biomolecules* **10** (1), 61 (2020). https://doi.org/10.3390/biom10010061

[39] **Sekhon-Loodu, S. and Rupasinghe, H.P.V.,** Evaluation of Antioxidant, Antidiabetic and Antiobesity Potential of Selected Traditional

Medicinal Plants. *Front. Nutr.*, **6**, 53 (2019). https://doi.org/10.3389/fnut.2019.00053

[40] **Mohamed, S.M., Shalaby, M.A., Al-Mokaddem, A.K., El-Banna, A.H., EL-Banna, H.A. and Nabil, G.,** Evaluation of anti-Alzheimer activity of Echinacea purpurea extracts in aluminum chloride-induced neurotoxicity in rat model. *J. Chem. Neuroanat.*, **128**, 102234 (2023). https://doi.org/10.1016/j.jchemneu.2023.102234

[41] **García-Ayllón, M.-S., Small, D.H., Avila, J. and Sáez-Valero, J.,** Revisiting the role of acetylcholinesterase in Alzheimer's disease: cross-talk with P-tau and β-amyloid. *Front. Mol. Neurosci.*, **4,** 22 (2011). https://doi.org/10.3389/fnmol.2011.00022

[42] **Mezgebe, K. and Mulugeta, E.,** Synthesis and pharmacological activities of azo dye derivatives incorporating heterocyclic scaffolds: a review. *RSC Adv.* **12** (40), 25932-25946 (2022). https://doi.org/10.1039/D2RA04934A

[43] **Ahmed, A.A.M., Mekky, A.E.M. and Sanad, S.M.H.,** New piperazine-based bis(thieno[2,3-b]pyridine) and bis(pyrazolo[3,4-b]pyridine) hybrids linked to benzofuran units: Synthesis and in vitro screening of potential acetylcholinesterase inhibitors. *Synth. Commun*., **52** (6), 912-925 (2022). https://doi.org/10.1080/00397911.2022.2056853

[44] **Al-Wasidi, A.S., Hassan, A.S. and Naglah, A.M.,** *In vitro* cytotoxicity and drug-likeness of pyrazolines and pyridines bearing benzofuran moiety. *J. Appl. Pharm. Sci.*, **10** (4), 142-148 (2020). https://doi.org/10.7324/JAPS.2020.104018

[45] **Hassan, A.S.,** Antimicrobial evaluation, *in silico* ADMET prediction, molecular docking, and molecular electrostatic potential of pyrazole-isatin and pyrazole-indole hybrid molecules. *J. Iran. Chem. Soc.*, **19** (8), 3577-3589 (2022). https://doi.org/10.1007/s13738-022-02551-6

[46] **Mortelmans, K. and Zeiger, E.,** The Ames Salmonella/microsome mutagenicity assay. *Mutat. Res., Fundam. Mol. Mech. Mutagen.*, **455** (1-2), 29-60 (2000). https://doi.org/10.1016/S0027-5107(00)00064-6

[47] **Garrido, A., Lepailleur, A., Mignani, S.M., Dallemagne, P. and Rochais, C.,** hERG toxicity assessment: Useful guidelines for drug design. *Eur. J. Med. Chem.*, **195**, 112290 (2020). https://doi.org/10.1016/j.ejmech.2020.112290

[48] **Di Martino, V., Verhoeven, D.W., Verhoeven, F., Aubin, F., Avouac, J., Vuitton, L., Lioté, F., Thévenot, T. and Wendling, D.,** Busting the myth of methotrexate chronic hepatotoxicity. *Nat. Rev. Rheumatol*., **19**, 96-110 (2023). https://doi.org/10.1038/s41584-022-00883-4

[49] **Prieto, P., Pineda, M. and Aguilar, M.,** Spectrophotometric quantitation of antioxidant capacity through the formation of a phosphomolybdenum complex: specific application to the determination of vitamin E. *Anal. Biochem.*, **269** (2), 337-341 (1999). https://doi.org/10.1006/abio.1999.4019

[50] **Oyaizu, M.,** Studies on Products of Browning Reaction - Antioxidative Activities of Products of Browning Reaction Prepared from Glucosamine. *Jpn. J. Nutr. Diet.*, **44** (6), 307-315 (1986). https://doi.org/10.5264/eiyogakuzashi.44.307

[51] **Rahman, M.M., Islam, M.B., Biswas, M. and Khurshid Alam, A.H.M.,** *In vitro* antioxidant and free radical scavenging activity of different parts of Tabebuia pallida growing in Bangladesh. *BMC Res. Notes* **8**, 621 (2015). https://doi.org/10.1186%2Fs13104-015-1618-6

[52] **Arnao, M. B., Cano, A. and Acosta, M.,** The hydrophilic and lipophilic contribution to total antioxidant activity. *Food Chem.*, **73,** 239-244 (2001). https://doi.org/10.1016/S0308-8146(00)00324-1

[53] **Wickramaratne, M.N., Punchihewa, J. C. and Wickramaratne, D. B. M.,** *In-vitro* alpha amylase inhibitory activity of the leaf extracts of *Adenanthera pavonina*. *BMC Complementary Altern. Med.*, **16**, 466 (2016). https://doi.org/10.1186/s12906-016-1452-y

[54] **Ellman, G.L., Courtney, K.D., Andres, V. and Featherstone, R. M.,** A new and rapid colorimetric determination of acetylcholinesterase activity. *Biochem. Pharmacol.*, **7**, 88-95 (1961). https://doi.org/10.1016/0006-2952(61)90145-9

[55] **Shivanand, P.,** Arthritis an autoimmune disorder: Demonstration of *In-vivo* anti-arthritic activity. *Int. J. Pharm. Life Sci.*, **1**, 38-43 (2010)

[56] **Soni, D. and Sureshkumar, P.,** Effect of methanolic root extract of Blepharispermum subsesssile DC in controlling arthritic activity. *Res. J. Biotechnol.*, **11** (4), 65-74 (2016).

[57] **Meera, S., Ramaiah, N. and Kalidindi, N.,** Illustration of anti-rheumatic mechanism of rheumavedic capsule. *Saudi Pharm. J.*, **19** (4), 279-284 (2011). https://doi.org/10.1016/j.jsps.2011.07.002

[58] **Oyedapo, O.O. and Famurewa, A. J.,** Antiprotease and Membrane Stabilizing Activities of Extracts of Fagara Zanthoxyloides, Olax Subscorpioides and Tetrapleura Tetraptera. *Int. J. Pharmacogn.*, **33** (1), 65-69 (1995). https://doi.org/10.3109/13880209509088150

[59] **Khatab, T.K., Kandil, E.-E.-D.M., Elsefy, D.E. and El-Mekabaty, A.,** A One-Pot Multicomponent Catalytic Synthesis of New 1*H*-Pyrazole-1-Carbothioamide Derivatives with Molecular Docking Studies as COX-2 Inhibitors. *Biointerface Res. Appl. Chem.*, **11** (6), 13779-13789 (2021). https://doi.org/10.33263/BRIAC116.1377913789

[60] **Soliman, H.A. and Khatab, T.K.,** New approach for tetrachlorosilane promoted one pot, condensation reaction for tetrahydrobenzo[*a*]xanthene-11-ones with docking validation as aurora kinase inhibitor *Silicon* **10** (2), 229-233 (2018). https://doi.org/10.1007/s12633-016-9421-0

[61] **Khatab, T.K., Mubarak, A.Y. and Soliman, H.A.,** Design and Synthesis Pairing Between Xanthene and Tetrazole in Pentacyclic System Using Tetrachlorosilane with Aurora Kinase Inhibitor Validation *J. Heterocycl. Chem.*, **54** (4), 2463-2470 (2017). https://doi.org/10.1002/jhet.2846